Spectroscopy of ^{155}Yb: Structure evolution in the $N = 85$ isotones

X. Q. Li (李湘庆),[1] C. Xu (徐川),[1,*] S. Q. Zhang (张双全),[1] H. Hua (华辉),[1,†] J. Meng (孟杰),[1] R. A. Bark,[2] Q. B. Chen (陈启博),[1] C. Y. Niu (牛晨阳),[1] R. Han (韩蕊),[1] S. M. Wyngaardt,[3] S. Y. Wang (王守宇),[4] S. Wang (王硕),[4] B. Qi (亓斌),[4] L. Liu (刘雷),[4] L. H. Zhu (竺礼华),[5] Z. Shi (施智),[5] G. L. Zhang (张高龙),[5] B. H. Sun (孙保华),[5] X. Y. Le (乐小云),[5] C. Y. Song (宋春燕),[5] Y. L. Ye (叶沿林),[1] D. X. Jiang (江栋兴),[1] F. R. Xu (许甫荣),[1] Z. H. Li (李智焕),[1] J. J. Sun (孙君杰),[1] Y. Shi (石跃),[1] P. W. Zhao (赵鹏巍),[1] W. Y. Liang (梁午阳),[1] C. G. Li (李晨光),[1] C. G. Wang (王春光),[1] X. C. Chen (陈潇驰),[1] Z. H. Li (李宗浩),[1] D. P. Sun (孙大鹏),[4] C. Liu (刘晨),[4] Z. Q. Li (李志泉),[4] P. Jones,[2] E. A. Lawrie,[2] J. J. Lawrie,[2] M. Wiedeking,[2] T. D. Bucher,[2,3] T. Dinoko,[2,6] B. V. Kheswa,[2,3] L. Makhathini,[2,3] S. N. T. Majola,[2,7] J. Ndayishimye,[2,3] S. P. Noncolela,[2,6] O. Shirinda,[2] J. Gál,[8] G. Kalinka,[8] J. Molnár,[8] B. M. Nyakó,[8] J. Timár,[8] K. Juhász,[9,‡] and M. Arogunjo[10]

[1]*School of Physics and State Key Laboratory of Nuclear Physics and Technology, Peking University, Beijing 100871, China*
[2]*iThemba LABS, P.O. Box: 722, Somerset West 7129, South Africa*
[3]*Department of Physics, University of Stellenbosch, Matieland 7602, South Africa*
[4]*Shandong Provincial Key Laboratory of Optical Astronomy and Solar-Terrestrial Environment, School of Space Science and Physics, Shandong University, Weihai 264209, China*
[5]*School of Physics and Nuclear Energy Engineering, Beihang University, Beijing 100191, China*
[6]*Department of Physics, University of the Western Cape, P/B X17, Bellville 7535, South Africa*
[7]*Department of Physics, University of Cape Town, Rondebosch 7700, South Africa*
[8]*Institute for Nuclear Research, Hungarian Academy of Sciences, H-4001 Debrecen, Hungary*
[9]*Department of Information Technology, University of Debrecen, H-4010 Debrecen, Hungary*
[10]*Department of Physics, Federal University of Technology, Akure (FUTA) Ondo State, Nigeria*

(Received 16 March 2016; published 24 August 2016)

High-spin states in ^{155}Yb have been studied via the ^{144}Sm(^{16}O,$5n$)^{155}Yb reaction at a beam energy of 118 MeV. One negative-parity and one positive-parity cascade built on the $\nu f_{7/2}$ and $\nu i_{13/2}$ states, respectively, are established for the first time. The structures observed in ^{155}Yb are compared with those in the neighboring $N = 85$ isotones and with semiempirical shell-model (SESM) calculations. According to adiabatic and configuration-fixed constrained triaxial covariant density functional theory (CDFT) calculations, a coexistence of prolate and oblate shapes is predicted to exist in ^{155}Yb.

DOI: 10.1103/PhysRevC.94.024337

I. INTRODUCTION

The light Yb isotopes around $A = 150$, which are situated in the transitional region between spherical and deformed nuclei, exhibit varied structural characteristics. For the even-even Yb isotopes, the low-lying excitations exhibit a clear structural evolution with neutron number N. For instance, with N decreasing from 88 to 84, ^{158}Yb shows the behavior of soft rotation [1]; ^{156}Yb undergoes an evolution from a quasivibrational to quasirotational structure with increasing spin [2,3]; and ^{154}Yb is interpreted in terms of the quasiparticle coupling [4,5]. For the odd-A Yb isotopes in this transitional region, collective structures built on the $f_{7/2}$, $h_{9/2}$, and $i_{13/2}$ neutron orbitals have been observed in ^{157}Yb [6,7] and the coexistence of different nuclear shapes has been revealed. With fewer valence neutrons outside the $N = 82$ closed shell, the structure information on ^{155}Yb is still scarce. Only one negative-parity cascade built on the $h_{9/2}$ orbital has been established in ^{155}Yb [8]. The excitations built upon the $(\nu f_{7/2})_{7/2^-}$ ground state and the low-lying $13/2^+$ state have not yet been observed in ^{155}Yb.

One thing worth mentioning is that, due to the neutron number of these transitional nuclei close to the octupole driving number 88 [9], the octupole degree of freedom is expected to play a role in their structures. Octupole 3^- states have been observed in the even-even nuclei around the $A \sim 150$ mass region [10–15]. For the $N = 85$ isotones ^{149}Gd, ^{151}Dy, and ^{153}Er, the low-lying positive-parity $13/2^+$ states have been described by a dominant $i_{13/2}$ configuration and a small mixing with the $3^- \otimes f_{7/2}$ excitation [16–18]. Thus, experimental investigations of the excitations built on the $f_{7/2}$ ground state and the low-lying $13/2^+$ state in ^{155}Yb would be very helpful for the systematic understanding of how the structure evolves in this transitional region.

Here, we present the results of a new investigation of ^{155}Yb. The new structures observed in ^{155}Yb are discussed in terms of comparison of systematics, and theoretical calculations by semiempirical shell-model (SESM) and the adiabatic and configuration-fixed constrained triaxial covariant density functional theory (CDFT).

II. EXPERIMENT AND RESULTS

The present experiment was performed at the separated sector cyclotron of iThemba LABS in South Africa. High-spin states in ^{155}Yb were populated by using the fusion-evaporation reaction ^{144}Sm(^{16}O,$5n$)^{155}Yb at a beam energy of 118 MeV.

*chuan@pku.edu.cn
†hhua@pku.edu.cn
‡Deceased.

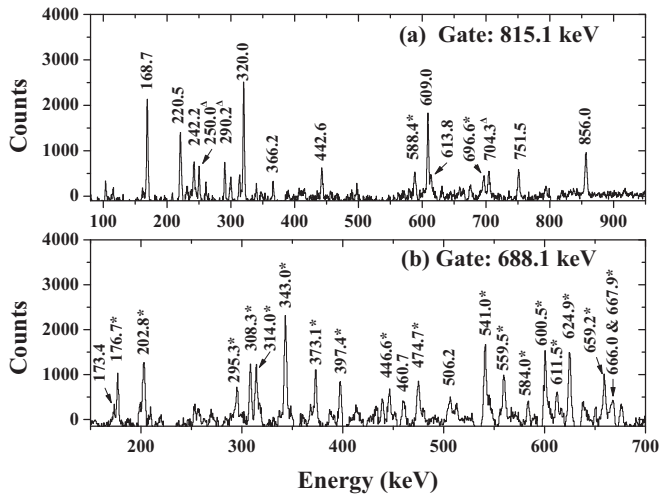

FIG. 1. Coincident γ-ray spectra gated on the (a) 815.1 keV and (b) 688.1 keV transitions. The peaks marked with stars are known contaminants from other nuclei, and the peaks marked with triangles are not included in the partial level scheme of Fig. 2.

The target consisted of a 2.89 mg/cm^2 ^{144}Sm metallic foil with a 13.13 mg/cm^2 Pb backing. The in-beam γ rays were measured with the AFRODITE array [19], which consists of eight Compton suppressed clover detectors at the time of the experiment. The clover detectors have been arranged in two rings at 90° (four clovers) and 135° (four clovers) with respect to the beam direction. To select specific reaction channels, the chessboard [20], comprising 24 CsI scintillators, was used in the present experiment.

A total of 1.03×10^{10} γ-γ coincident events were collected, from which a symmetric matrix was built. The level scheme analysis was performed by using the RADWARE package [21]. The γ-ray spectra gated on the 815.1 and 688.1 keV γ-ray transitions in ^{155}Yb are shown in Fig. 1. To determine the multipolarities of the γ-ray transitions, two asymmetric angular distributions from oriented states (ADO) [22] matrices were constructed by using the γ rays detected at all angles (y axis) against those detected at 90° and 135° (x axis), respectively. The multipolarities of the emitted γ rays were analyzed by means of the ADO ratio, which was defined as [I_γ (at 135°)]/[I_γ (at 90°)]. The typical ADO ratios for stretched quadrupole and stretched pure dipole transitions are found to be ∼1.2 and ∼0.8, respectively. The excitation energies, γ-ray energies, γ-ray transition intensities, ADO ratios, and spin-parity assignments for the ^{155}Yb nucleus are summarized in Table I. It is noted that a different normalization has been used for the γ rays belonging to the $7/2^-$ and $13/2^+$ sequences than for those feeding the $9/2^-$ state, due to the reason that some neighboring nuclei also have strong transitions with ∼666.0 keV.

The spectroscopy of ^{155}Yb has been previously studied via the ^{102}Pd(^{58}Ni ,4pn)^{155}Yb reaction by Ding *et al.* [8]. In that work, a low-lying negative-parity sequence up to spin $(21/2^-)$ at 1912.8 keV was established above the $9/2^-$ state, which feeds the $7/2^-$ ground state through the 168.7-keV line. The partial level scheme of ^{155}Yb deduced from the present work is shown in Fig. 2. It was constructed from the γ-γ coincidence relationships, intensity balances, and ADO analyses. The present analysis confirms the low-lying negative-parity levels above the $9/2^-$ state found in Ref. [8] and extends this sequence to the $33/2^-$ state at 3740.8 keV with the observation of three new γ-ray transitions of 856.0, 751.5,

TABLE I. γ-ray energies, excitation energies, relative γ-ray intensities, and ADO ratios in ^{155}Yb.

E_γ (keV)[a]	E_i (keV)	E_f (keV)	Int. (%)	ADO ratio	Assignment
168.7	168.7	0.0	37.7(6)	0.97(2)	$(9/2^-) \rightarrow 7/2^-$
173.4	839.4	666.0	98.2(54)[b]	0.76(1)	$(13/2^+) \rightarrow (11/2^-)$
220.5	3740.8	3520.3	32.5(6)	1.29(2)	$(33/2^-) \rightarrow (29/2^-)$
242.2	2768.8	2526.6	16.6(3)	0.95(2)	$(25/2^-) \rightarrow (23/2^-)$
317.8	983.8	666.0			$(13/2^-) \rightarrow (11/2^-)$
320.0	1912.8	1592.8	70.3(6)	1.38(2)	$(21/2^-) \rightarrow (17/2^-)$
349.0	1527.5	1178.5	71.5(25)[b]	0.86(2)	$(17/2^+) \rightarrow (15/2^-)$
366.2	4549.6	4183.4	15.9(2)	0.79(1)	$(37/2^-) \rightarrow (35/2^-)$
414.3	1592.8	1178.5			$(17/2^-) \rightarrow (15/2^-)$
442.6	4183.4	3740.8	20.8(4)	0.68(8)	$(35/2^-) \rightarrow (33/2^-)$
460.7	2494.4	2033.7	68.3(28)[b]	1.36(7)	$(25/2^+) \rightarrow (21/2^+)$
506.2	2033.7	1527.5	70.0(10)[b]	1.07(3)	$(21/2^+) \rightarrow (17/2^+)$
512.5	1178.5	666.0	75.4(26)[b]		$(15/2^-) \rightarrow (11/2^-)$
609.0	1592.8	983.8	80.2(14)	1.29(3)	$(17/2^-) \rightarrow (13/2^-)$
613.8	2526.6	1912.8	18.3(7)	0.67(2)	$(23/2^-) \rightarrow (21/2^-)$
666.0	666.0	0.0	178.8(54)[b]	1.28(3)	$(11/2^-) \rightarrow (7/2^-)$
688.1	1527.5	839.4	100[b]	1.24(7)	$(17/2^+) \rightarrow (13/2^+)$
751.5	3520.3	2768.8	35.2(7)	1.30(3)	$(29/2^-) \rightarrow (25/2^-)$
815.1	983.8	168.7	100	1.35(3)	$(13/2^-) \rightarrow (9/2^-)$
856.0	2768.8	1912.8	46.3(5)	1.01(3)	$(25/2^-) \rightarrow (21/2^-)$

[a]Uncertainties between 0.2 and 0.5 keV.
[b]Normalized to 688.1 keV transition.

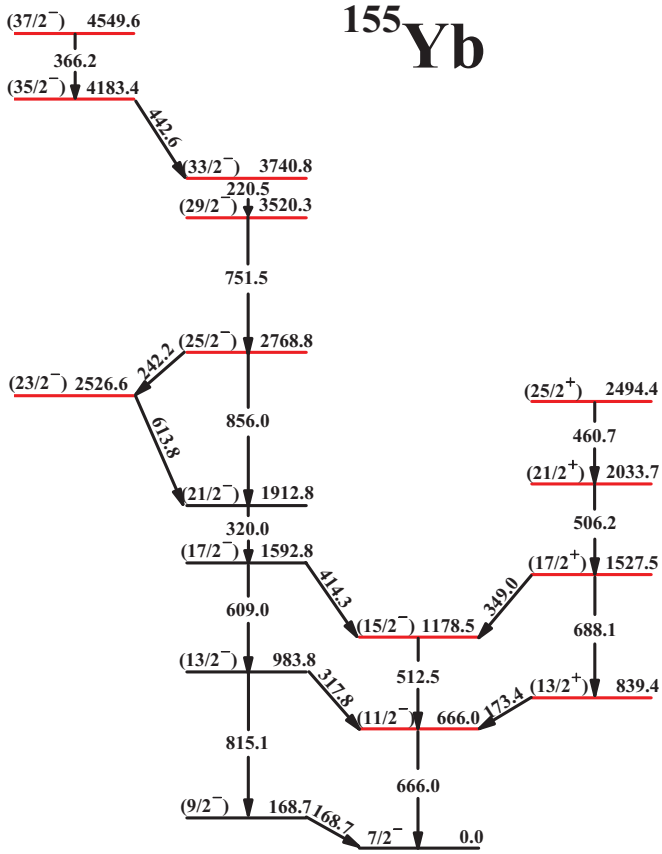

FIG. 2. Partial level scheme of ^{155}Yb. New levels are indicated by red lines.

and 220.5 keV, as shown in Fig. 1. The ADO ratio analyses suggest that the 751.5- and 220.5-keV γ-ray transitions have quadrupole characters. The ADO value of 856.0-keV transition is 1.01, considering that its side bypass 613.8-keV transition following the 242.2-keV transition was found to have relatively pure dipole character, so the 856.0-keV transition is the most likely to also have the quadrupole character and the side bypass 242.2-keV transition has the $M1/E2$ character based on their coincidence relationships, intensity balances, and ADO values. The 366.2-keV transition observed in Ref. [8] and a new 442.6-keV transition are found to have dipole natures and placed above the 3740.8 keV level.

A new negative-parity sequence, built on the $7/2^-$ ground state, is observed in the present work. The observation of 317.8- and 414.3-keV γ rays further confirms the placements of these levels. The ADO ratio analyses suggest that the 666.0-keV transition has quadrupole character. The γ-ray decay of 512.5 keV for which the ADO value could not be extracted is also assumed to be a stretched $E2$ transition. A new state with a spin-parity $13/2^+$ is placed at 839.4 keV in ^{155}Yb with the observation of a 173.4-keV transition linking it to the $11/2^-$ state at 666.0 keV. The present ADO analyses suggest a dipole nature for the 173.4-keV transition. Three new transitions of 688.1, 506.2, and 460.7 keV are found to be in coincidence with the 173.4- and 666.0-keV transitions and are placed above the 839.4 keV level. According to the ADO values obtained in the current work, quadrupole assignments are made for these three transitions.

III. DISCUSSION

The new level scheme obtained in the present study for ^{155}Yb, together with that known previously for neighboring nuclei, allows a systematic discussion of the low-lying intrinsic states of the even-Z isotones. The systematics of the excitation energies associated with the neutron $f_{7/2}$, $h_{9/2}$, and $i_{13/2}$ intrinsic states in the $N = 85$ and 87 isotones are plotted in Figs. 3(a) and 3(b), respectively. It can be seen in Fig. 3(b) that in the $N = 87$ isotones with the increase of proton number, both the excitation energies associated with the $\nu h_{9/2}$ and $\nu i_{13/2}$ intrinsic states decrease gradually. The underlying reason for this gradual decrease has been discussed in Ref. [7]. In this mass region, the strong attractive interaction between spin-orbit partner orbitals $\pi h_{11/2}$ and $\nu h_{9/2}$ as well as the relatively weaker attractive interaction between the $\pi h_{11/2}$ and $\nu i_{13/2}$ configurations will result in the onset of nuclear deformation [26]. With the increase of proton number, the increased occupation of $\pi h_{11/2}$ orbitals will gradually enhance the overall attractive proton-neutron interaction and lower the energies of the $\nu h_{9/2}$ and $\nu i_{13/2}$ orbitals.

For the $N = 85$ isotones, the excitation energies of the $\nu h_{9/2}$ orbital follow the same trend as $N = 87$ isotones, as shown in Fig. 3(a). However, the excitation energies of $13/2^+$ state in the $N = 85$ isotones are different from those in the $N = 87$ isotones. It remains almost constant with the increase of proton number until ^{153}Er. In Refs. [16–18,27], the low-lying $13/2^+$ states in ^{149}Gd, ^{151}Dy, and ^{153}Er were interpreted to be a dominant $\nu i_{13/2}$ configuration together with a small mixing from the $3^- \otimes f_{7/2}$ excitation.

In Figs. 3(c) and 3(d), the available excitation energies of the octupole 3^- states in the neighboring even-even $N = 84$ and 86 isotones are plotted [10–15], respectively. Until now, low-lying 3^- states in three isotones of $N = 84$ (^{148}Gd, ^{150}Dy, and ^{152}Er) and two of $N = 86$ (^{150}Gd and ^{152}Dy) have been observed. It can be seen that their excitation energies increase with proton number. Therefore, the mixture of the $\nu i_{13/2}$ intrinsic state and the $3^- \otimes f_{7/2}$ excitation would result in almost constant excitation energies of the $13/2^+$ states in ^{149}Gd, ^{151}Dy, and ^{153}Er. By contrast, the excitation energy of the $13/2^+$ state in ^{155}Yb decreases significantly compared with that of the neighboring isotone ^{153}Er and is similar to the decrease pattern of the $13/2^+$ states in the $N = 87$ isotones. This indicates that the $13/2^+$ state in ^{155}Yb may have a purer $\nu i_{13/2}$ configuration than those in the light neighboring $N = 85$ isotones and that the contribution to the $13/2^+$ state originating from the octupole 3^- state coupled to the odd particle in the $f_{7/2}$ orbital is small above proton number $Z = 68$. It is consistent with the lack of evidence for 3^- states in ^{154,156}Yb at present. So far, the low-lying $13/2^+$ state in ^{157}Hf has not yet been observed. Whether its excitation energy follows the systematics of the even-Z $N = 87$ isotones is an interesting question.

The nuclear shape of the transitional Yb isotopes is soft and influenced by the nature of the intrinsic orbitals. To investigate the polarization effects of the neutron $f_{7/2}$, $h_{9/2}$, and $i_{13/2}$

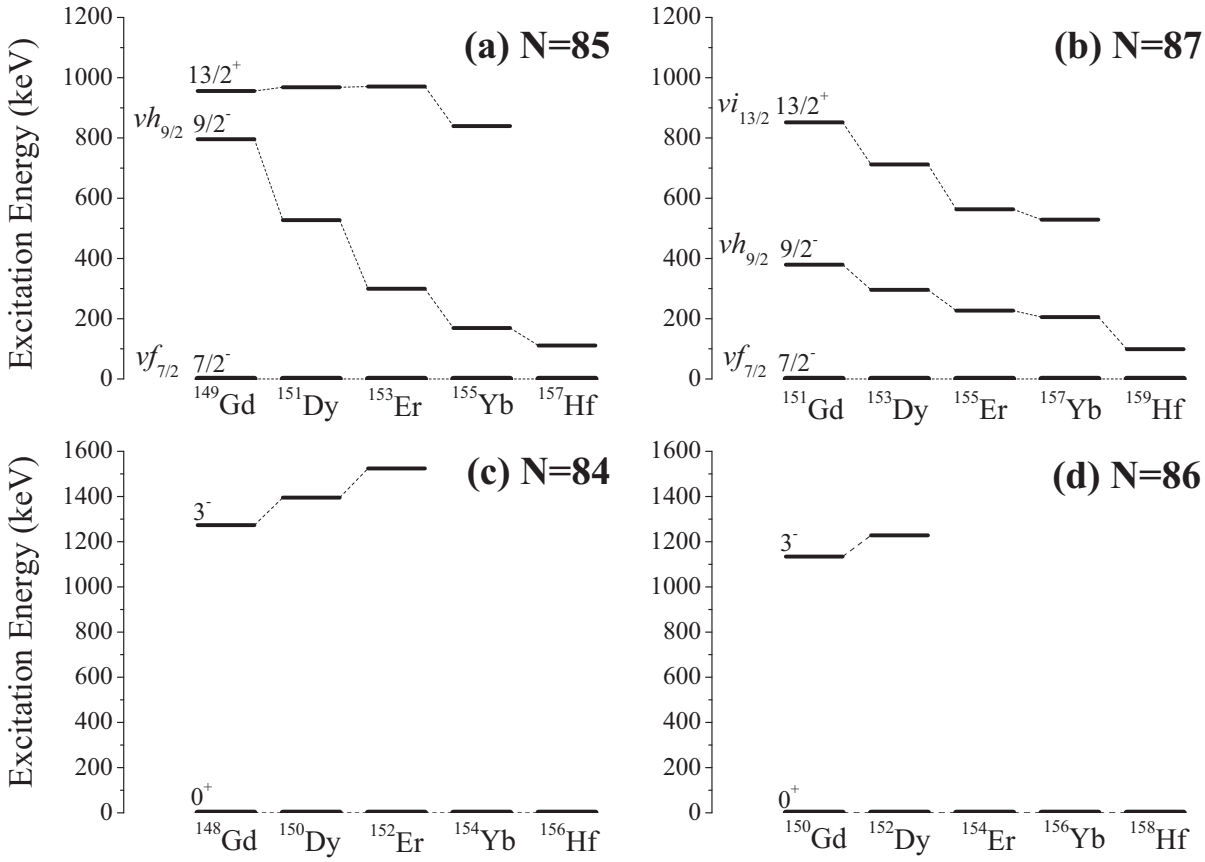

FIG. 3. Systematics of known excitations associated with the (a) $\nu f_{7/2}$, $\nu h_{9/2}$, and $\nu i_{13/2}$ states, in the $N = 85$ even-Z isotones; (b) $\nu f_{7/2}$, $\nu h_{9/2}$, and $\nu i_{13/2}$ intrinsic states in the $N = 87$ even-Z isotones; (c) 3^- excitations in the $N = 84$ even-even isotones; (d) 3^- excitations in the $N = 86$ even-even isotones. Data are taken from Refs. [7,10–18,23–25] and the present work.

orbitals on the nuclear shape, adiabatic and configuration-fixed constrained triaxial CDFT calculations [28–31] with the newly proposed point-coupling energy density functional PC-PK1 [32] have been performed. The calculated potential-energy surface (PES) in the β-γ plane ($0^\circ \leqslant \gamma \leqslant 60^\circ$) for ^{155}Yb is shown in Fig. 4. All energies are normalized with respect to the binding energy of the absolute minimum, and the energy separation between contour lines is 0.2 MeV. It

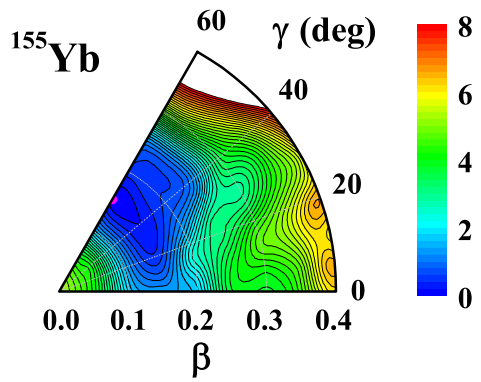

FIG. 4. The potential-energy surface in the β-γ plane ($0^\circ \leqslant \gamma \leqslant 60^\circ$) for ^{155}Yb calculated by constrained triaxial CDFT with a newly proposed point-coupling energy density functional PC-PK1. The energy separation between each contour line is 0.2 MeV.

can be seen that the ground state of ^{155}Yb is oblate with $\beta = 0.15$. Around the minimum, the PES exhibits a relatively soft character along the direction of γ. The configuration of the ground state in ^{155}Yb is predicted to be $\nu f_{7/2}$, which is consistent with the previous assignment for the $7/2^-$ ground state. According to the configuration-fixed constrained CDFT calculations, the $(\nu h_{9/2})_{9/2^-}$ state is prolate with $\beta = 0.14$, while the $(\nu i_{13/2})_{13/2^+}$ state is oblate with $\beta = 0.16$. Thus, a coexistence of different shapes is predicted to exist in the transitional ^{155}Yb nucleus.

With three neutrons outside the $N = 82$ closed shell, the low-lying excitations of transitional ^{155}Yb might exhibit a pattern of multiparticle levels formed by coupling the odd nucleon to the even-even core excitations. Indeed, in the $N = 85$ isotones ^{153}Er, ^{151}Dy, and ^{149}Gd, such a pattern of multiparticle levels has been revealed [16–18]. In Fig. 5, the excited states built on different orbitals in ^{155}Yb are compared with the positive-parity yrast states in the corresponding $N = 84$ ^{154}Yb core. The positive-parity yrast structure of the ^{154}Yb core has been described by using the $\nu(f_{7/2})^2$ configuration for levels from 0^+ to 6^+ [33]. Here, the similarity of excitation energies between ^{154}Yb and ^{155}Yb suggests that the excited structure of ^{155}Yb can also be well explained in terms of multiparticle excitation.

To further illustrate the excitation pattern of ^{155}Yb, semiempirical shell-model (SESM) calculations are also performed.

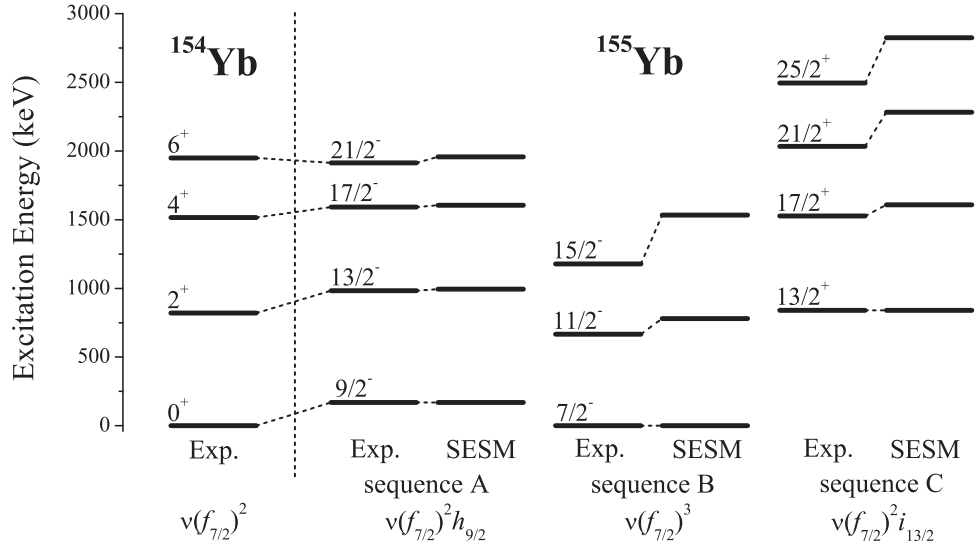

FIG. 5. Experimental and theoretical systematics of excited states in ^{154,155}Yb.

The SESM is usually applied to nuclei close to the major closed shell where multiparticle excitations dominate. In this approach, level energies of multiparticle-hole configurations are calculated by using nuclear ground-state masses, single-particle energies, and two-particle interactions obtained from experimental data in the neighboring nuclei. The detailed description of SESM can be found in Ref. [34] and references therein. In the present calculations, ^{154}Yb was chosen as the core. The calculations were performed in the model space $\nu(h_{9/2},\ f_{7/2},\ i_{13/2})$ and two-body interactions were taken into account. The single particle energies and the two-body interactions were extracted from the neighboring nuclei ^{154}Yb [5], ^{153}Er [18], ^{152}Er [35], and the present work.

Taking the $13/2^-$ state in ^{155}Yb as an example, its main configuration is $\nu h_{9/2} \otimes {}^{154}\mathrm{Yb}(2^+)$, and its excitation energy is calculated as

$$\begin{aligned} &E(^{155}\mathrm{Yb};13/2^-;\nu h_{9/2}\otimes 2^+)\\ &\quad = E(^{154}\mathrm{Yb};2^+) + E(^{155}\mathrm{Yb};9/2^-;\nu h_{9/2})\\ &\qquad + S + \Delta(\nu h_{9/2}\otimes 2^+)\\ &\quad = 994.3\ \mathrm{keV}, \end{aligned} \tag{1}$$

where E is the corresponding level energy and Δ is the two-body interaction. The Δ can be extracted from the neighboring nuclei as follows:

$$\begin{aligned} \Delta(\nu h_{9/2}\otimes 2^+) = {}& E(^{153}\mathrm{Er};13/2^-;\nu h_{9/2}\otimes 2^+) - E(^{152}\mathrm{Er};2^+)\\ & - E(^{153}\mathrm{Er};9/2^-;\nu h_{9/2}) - S'. \end{aligned} \tag{2}$$

In this case, the binding-energy terms S and S' are equal to zero. The SESM-calculated energy levels for ^{155}Yb are compared with the experimental levels in Fig. 5. As seen in Fig. 5, the SESM calculations excellently reproduce the experimental excitation energies of level sequence A, and reasonably reproduce those of level sequences B and C. The good agreement between the SESM calculations and experimental data further confirm that multiparticle excitations dominate the low-lying levels in ^{155}Yb. With increasing spin, the SESM calculations overestimate the experimental excitation energy of the states in sequences B and C. As shown in the formula (1), the calculated level energies of ^{155}Yb depend on the characters of the excited states of ^{154}Yb core which are sensitive to its shape. Since the ^{154}Yb core was predicted to have moderately prolate [36] which is similar to the prolate shape of $(\nu h_{9/2})_{9/2^-}$ state of ^{155}Yb but different from the oblate shapes of $(\nu f_{7/2})_{7/2^-}$ and $(\nu i_{13/2})_{13/2^+}$ states, the shape effect may be the underlying reason for the good agreement obtained for the level sequence A, and overestimation for level sequences B and C.

IV. SUMMARY

With the ^{16}O beam provided by iThemba LABS, high-spin states of ^{155}Yb have been studied via the ^{144}Sm(^{16}O ,5n)^{155}Yb fusion-evaporation reaction. A previously known cascade built on the $\nu h_{9/2}$ orbital is extended up to the higher spin state $33/2^-$. One negative-parity and one positive-parity cascade built on the $\nu f_{7/2}$ and $\nu i_{13/2}$ states, respectively, have been identified for the first time. The structural characters observed in ^{155}Yb are studied in comparison with similar structures in the neighboring $N = 84$–87 isotones and SESM calculations. It is proposed that the low-lying $13/2^+$ states in ^{155}Yb have a purer $i_{13/2}$ configuration than those in the light $N = 85$ isotones and that the multiparticle excitation provides a good description of the low-lying excited states in ^{155}Yb. The adiabatic and configuration-fixed constrained triaxial CDFT calculations indicate that the $(\nu f_{7/2})_{7/2^-}$ ground state and the $(\nu i_{13/2})_{13/2^+}$ state of ^{155}Yb have a similar oblate shape with $\gamma \sim 60^\circ$, while the $(\nu h_{9/2})_{9/2^-}$ state has a prolate shape with $\gamma \sim 0^\circ$. Based on these, a shape coexistence is suggested to occur in the nucleus ^{155}Yb.

ACKNOWLEDGMENTS

This work is supported by the Natural Science Foundation of China under Grants No. 11175003, No. 11235001, No. 11335002, No. 11320101004, No. 11375017, No. 11375015,

No. 11575006, No. J1103206, No. 11461141001, and No. 11461141002, the Chinese Major State Basic Research Development Program under Grant No. 2013CB834400, and the SA/CHINA research collaboration in science and technology under Grant No. CS05-L06. The authors wish to thank Dr. Q. W. Fan for making the target and the iThemba LABS technical staff and accelerator group for their support and for providing the beam.

[1] S. B. Patel, F. S. Stephens, J. C. Bacelar, E. M. Beck, M. A. Deleplanque, R. M. Diamond, and J. E. Draper, Phys. Rev. Lett. **57**, 62 (1986).
[2] C. J. Lister, D. Horn, C. Baktash, E. der Mateosian, O. C. Kistner, and A. W. Sunyar, Phys. Rev. C **23**, 2078 (1981).
[3] Z. Y. Li, H. Hua, S. Y. Wang, J. Meng, Z. H. Li, X. Q. Li, F. R. Xu, H. L. Liu, S. Q. Zhang, Y. L. Ye, D. X. Jiang, T. Zheng, L. Y. Ma, F. Lu, F. Y. Fan, L. Y. Han, H. Wang, J. Xiao, D. Chen, X. Fang, J. L. Lou, S. G. Zhou, L. H. Zhu, X. G. Wu, G. S. Li, C. Y. He, Y. Liu, X. Q. Li, X. Hao, B. Pan, and L. H. Li, Phys. Rev. C **77**, 064323 (2008).
[4] K. S. Vierinen, A. A. Shihab-Eldin, J. M. Nitschke, P. A. Wilmarth, R. M. Chasteler, R. B. Firestone, and K. S. Toth, Phys. Rev. C **38**, 1509 (1988).
[5] C. T. Zhang, R. Broda, R. Menegazzo, P. Kleinheinz, R. Collatz, H. Grawe, S. Hofmann, M. Lach, K. H. Maier, M. Schramm, R. Schubart, and J. Blomqvist, Z. Phys. A **345**, 327 (1993).
[6] Y. Zheng, X. H. Zhou, Y. H. Zhang, Y. X. Guo, X. G. Lei, Z. Liu, J. J. He, M. L. Liu, W. J. Luo, S. X. Wen, L. H. Zhu, and C. X. Yang, Eur. Phys. J. A **14**, 133 (2002).
[7] C. Xu, H. Hua, X. Q. Li, J. Meng, Z. H. Li, F. R. Xu, Y. Shi, H. L. Liu, S. Q. Zhang, Z. Y. Li, L. H. Zhu, X. G. Wu, G. S. Li, C. Y. He, S. G. Zhou, S. Y. Wang, Y. L. Ye, D. X. Jiang, T. Zheng, J. L. Lou, L. Y. Ma, E. H. Wang, Y. Y. Cheng, and C. He, Phys. Rev. C **83**, 014318 (2011).
[8] K. Y. Ding, J. A. Cizewski, D. Seweryniak, H. Amro, M. P. Carpenter, C. N. Davids, N. Fotiades, R. V. F. Janssens, T. Lauritsen, C. J. Lister, D. Nisius, P. Reiter, J. Uusitalo, I. Wiedenhöver, and A. O. Macchiavelli, Phys. Rev. C **64**, 034315 (2001).
[9] W. Nazarewicz, P. Olanders, I. Ragnarsson, J. Dudek, G. A. Leander, P. Möller, and E. Ruchowsa, Nucl. Phys. A **429**, 269 (1984).
[10] K. S. Toth, D. C. Sousa, J. M. Nitschke, and P. A. Wilmarth, Phys. Rev. C **35**, 310 (1987).
[11] S. Lunardi, P. Kleinheinz, M. Piiparinen, M. Ogawa, M. Lach, and J. Blomqvist, Phys. Rev. Lett. **53**, 1531 (1984).
[12] M. Piiparinen, P. Kleinheinz, S. Lunardi, M. Ogawa, G. Angelis, F. Soramel, W. Meczynski, and J. Blomqvist, Z. Phys. A **337**, 387 (1990).
[13] J. Styczen, Y. Nagai, M. Piiparinen, A. Ercan, and P. Kleinheinz, Phys. Rev. Lett. **50**, 1752 (1983).
[14] A. Algora *et al.* (GSI Euroball Collaboration), Phys. Rev. C **68**, 034301 (2003).
[15] D. R. Hacnni and T. T. Sugihara, Phys. Rev. C **16**, 120 (1977).
[16] M. Piiparinen, R. Pengo, Y. Nagai, E. Hammarén, P. Kleinheinz, N. Roy, L. Carlén, H. Ryde, Th. Lindblad, A. Johnson, S. A. Hjorth, and J. Blomqvist, Z. Phys. A **300**, 133 (1981).
[17] M. Piiparinen, S. Lunardi, P. Kleinheinz, H. Backe, and J. Blomqvist, Z. Phys. A **290**, 337 (1979).
[18] C. Foin, F. Farget, A. Gizon, D. Santos, D. Barnéoud, J. Genevey, J. Gizon, P. Paris, M. Ashgar, and A. Płochocki, Eur. Phys. J. A **7**, 149 (2000).
[19] J. F. Sharpey-Schafer, Nucl. Phys. News **14**, 5 (2004).
[20] F. S. Komati, R. A. Bark, J. Gál, E. Gueorguieva, K. Juhász, G. Kalinka, A. Krasznahorkay, J. J. Lawrie, M. Lipoglavšek, M. Maliage, J. Molnár, S. M. Mullins, S. H. T. Murray, B. M. Nyakó, M. Ramashidza, J. F. Sharpey-Schafer, J. N. Scheurer, J. Timár, P. Vymers, and L. Zolnai, AIP Conf. Proc. **802**, 215 (2005).
[21] D. C. Radford, Nucl. Instrum. Methods Phys. Res., Sect. A **361**, 297 (1995).
[22] M. Piiparinen, A. Ataç, J. Blomqvist, G. B. Hagemann, B. Herskind, R. Julin, S. Juutinen, A. Lampinen, J. Nyberg, G. Sletten, P. Tikkanen, S. Törmänen, A. Virtanen, and R. Wyss, Nucl. Phys. A **605**, 191 (1996).
[23] A. F. Saad, C. T. Zhang, R. Collatz, P. Kleinheinz, R. Menegazzo, R. Broda, K. H. Maier, H. Grawe, M. Schramm, R. Schubart, M. Lach, J. Heese, J. Eberth, W. Krolas, S. Hofmann, H. Folger, and J. Blomqvist, Z. Phys. A **351**, 247 (1995).
[24] P. Kleinheinz, A. M. Stefanini, M. R. Maier, R. K. Sheline, R. M. Diamond, and F. S. Stephens, Nucl. Phys. A **283**, 189 (1977).
[25] K. Y. Ding, J. A. Cizewski, D. Seweryniak, H. Amro, M. P. Carpenter, C. N. Davids, N. Fotiades, R. V. F. Janssens, T. Lauritsen, C. J. Lister, D. Nisius, P. Reiter, J. Uusitalo, I. Wiedenhöver, and A. O. Macchiavelli, Phys. Rev. C **62**, 034316 (2000).
[26] R. F. Casten, D. D. Warner, D. S. Brenner, and R. L. Gill, Phys. Rev. Lett. **47**, 1433 (1981).
[27] N. Mansour, T. Bayomy, Z. Awwad, and M. Hossein, Appl. Radiat. Isot. **41**, 307 (1990).
[28] J. Meng, J. Peng, S. Q. Zhang, and S.-G. Zhou, Phys. Rev. C **73**, 037303 (2006).
[29] J. Peng, H. Sagawa, S. Q. Zhang, J. M. Yao, Y. Zhang, and J. Meng, Phys. Rev. C **77**, 024309 (2008).
[30] J. M. Yao, B. Qi, S. Q. Zhang, J. Peng, S. Y. Wang, and J. Meng, Phys. Rev. C **79**, 067302 (2009).
[31] J. Li, S. Q. Zhang, and J. Meng, Phys. Rev. C **83**, 037301 (2011).
[32] P. W. Zhao, Z. P. Li, J. M. Yao, and J. Meng, Phys. Rev. C **82**, 054319 (2010).
[33] C. T. Zhang, P. Kleinheinz, M. Piiparinen, R. Broda, R. Collatz, P. J. Daly, K. H. Maier, R. Menegazzo, G. Sletten, J. Styczen, and J. Blomqvist, Phys. Rev. C **54**, R1 (1996).
[34] J. Blomqvist and L. Rydström, Phys. Scr. **31**, 31 (1985).
[35] A. Kuhnert, D. Alber, H. Grawe, H. Kluge, K. H. Maier, W. Reviol, X. Sun, E. M. Beck, A. P. Byrne, H. Hübel, J. C. Bacelar, M. A. Deleplanque, R. M. Diamond, and F. S. Stephens, Phys. Rev. C **46**, 484 (1992).
[36] G. A. Lalazissis, S. Raman, and P. Ring, At. Data Nucl. Data Tables **71**, 1 (1999).